CILAMCE 2017
Florianópolis - Santa Catarina - Brazil

DYNAMIC MODELING AND CONTROL OF A QUADCOPTER WITH LONGITUDINAL-TILTING ROTORS

Henrique Bezerra Diógenes

hbd.ita@gmail.com

Davi Antônio dos Santos

davists@ita.br

Instituto Tecnológico de Aeronáutica

São José dos Campos, Brazil 12228-900

Abstract. *The present paper investigates a quadrotor vehicle with rotors that can be continuously commanded to tilt in one degree of freedom, frontward and backward. In particular, we are concerned here with the dynamic modeling and flight control design for the new multirotor vehicle. To model the vehicle's dynamics, this work adopts the Newton-Euler approach, considering its motion in six degrees of freedom and accounting for a first-order dynamics in the tilting mechanism. The flight control system is designed based on the time-scale separation between the attitude and position dynamics, being the first the fastest one. In this case, the attitude and position control laws are designed separately using feedback linearization combined with proportional and derivative actions and control saturation. Finally, we generate the commanded trajectory so as to make the vehicle follow a waypoint-based path with a desired speed and with its longitudinal axis pointing toward the next waypoint of the sequence. An extensive simulation study is carried out to assess the dynamics behavior of the new multirotor vehicle on different desired speed and tilting mechanism dynamics. The results show that the vehicle can be effectively controlled to stay almost aligned with the horizontal plane during all the trajectory.*

Keywords: *Multirotor aerial vehicle, flight control system, nonlinear control.*

1 INTRODUCTION

The multirotor aerial vehicles (MAVs) have become more and more popular in the last fifteen years both in academic and industrial applications. Conventional MAVs require a controlled attitude motion in order to suitably direct the resulting thrust force to produce lateral acceleration for position tracking Mahony et al. (2012); Santos et al. (2013); H.Bouadi et al. (2007); Pounds (2007). Occasionally, a wide attitude motion is undesirable, e.g., for maintaining a camera with its optical axis almost aligned with the local vertical, or for saving energy when dealing with high-inertia vehicles.

There are some authors that use structural modifications to improve the flight performance of MAVs. Escareno et al. Escareno et al. (2008) show how to design the attitude control laws for a tri-rotor MAV using nested saturation control. All the three rotors of this MAV have a one-degree-of-freedom (DOF) tilting mechanism. The vehicle shows an improved maneuverability compared to conventional quadcopter. Mohamed and Lanzon Mohamed and Lanzon (2012) investigated a tri-rotor MAV similar to the above-described one; for the flight control, this work adopt an H_∞ loop-shaping controller for both attitude and position tracking. Segui-Gasco et al. Segui-Gasco et al. (2014) proposes a strategy that uses a dual axis tilting propeller to offer a wider range of control torques. Oner et al. Oner et al. (2008) presented a quadrotor MAV which tilts its rotors from vertical position to horizontal in such a way that it can take-off and land vertically like a helicopter and fly horizontally like an airplane. Efraim et al. (2015) investigated the effects of tilting inwards the plane of rotation of the vehicle's rotors, showing that it can improve the vehicle's stability.

The present paper investigates the dynamics and flight control of a quadrotor vehicle with one-degree-of-freedom longitudinal tilting rotors. The longitudinal translational motion is controlled by continuously actuating via the tilting mechanism, while the lateral translation as well as the attitude motion are stabilized by differential thrust, as in the conventional MAVs. In this case, the rotor plane remains stabilized in the horizontal plane during forward cruise flights without lateral disturbances. Additionally, the MAV under investigation is commanded to follow a waypoint position trajectory with its frontal side pointing towards the next waypoint.

The contributions of this paper are:

1. dynamic modeling of a quadrotor vehicle with longitudinal tilting rotors;
2. investigation of control strategies for the new quadrotor configuration;
3. trajectory generation to follow a waypoint-based path in such a way that the airframe stays almost aligned with the local horizontal;
4. simulation of the flight control system of the new MAV in nominal conditions.

The remaining text is organized in the following manner. Section 2 derives the dynamic model of an MAV with an one-degree-of-freedom longitudinal-tilting rotors. Section 3 formulates the attitude and position control laws and the control allocation strategies. Section 4 evaluates the proposed control system using computer simulation in nominal conditions. Finally, Section 5 concludes the paper.

2 DYNAMIC MODELING

Figure 1 shows two Cartesian coordinate systems (CCS) and illustrates the MAV with tilting rotors. The Body CCS $\mathcal{S}_{\mathrm{B}} \triangleq \{\mathrm{X_B}, \mathrm{Y_B}, \mathrm{Z_B}\}$ is fixed on the vehicle's structure at its center of mass (CM). The Ground CCS $\mathcal{S}_{\mathrm{G}} \triangleq \{\mathrm{X_G}, \mathrm{Y_G}, \mathrm{Z_G}\}$ is fixed on the ground at a known point O. The MAV consists in a quadrotor helicopter with rotors in an H configuration and with a tilting DOF (the angle α) around $\mathrm{Y_B}$. The thrust force and reaction torque of each propeller are denoted by f_i and τ_i, respectively, for $i = 1, 2, 3, 4$.

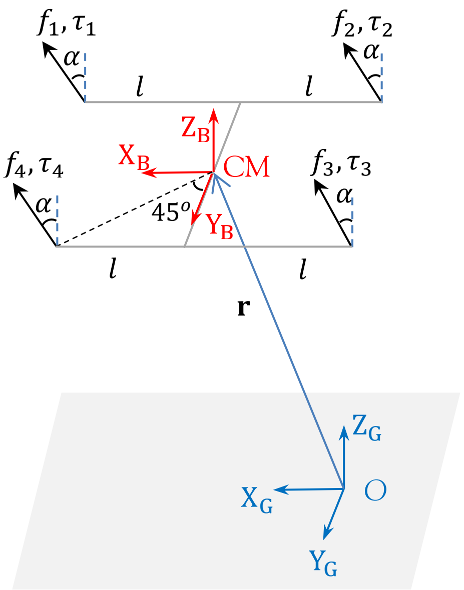

Figure 1: Schematic illustration of the quadcopter with tilting rotors.

2.1 Effectors

The thrust force f_i and reaction torque τ_i produced by each rotor in the vehicle's body are modeled by

$$f_i = k_f \omega_i^2, \tag{1}$$

$$\tau_i = k_\tau \omega_i^2, \tag{2}$$

for $i = 1, ..., 4$, where ω_i is the rotation speed of the ith rotor, k_f is the force coefficient, and k_τ is the torque coefficient. The coefficients k_f and k_τ depend on the air density, blade geometry, angle of attack, and air speed; they can be obtained by wind tunnel experiments.

On the other hand, the rotation speed ω_i of the ith rotor is modeled by the the follwing first order linear model:

$$\frac{\omega_i(s)}{\bar{\omega}_i(s)} = \frac{k_m}{\tau_m s + 1}, \tag{3}$$

where $\bar{\omega}_i(s)$ is a speed command, k_m is a DC gain, and τ_m is a time constant. The parameters k_m and τ_m can be obtained experimentally by simple bench tests Bouabdallah and Siegwart (2005).

In this paper, we assume that the tilting actuation mechanism can be modeled by a first order linear dynamic system

$$\frac{\alpha(s)}{\bar{\alpha}(s)} = \frac{k_\alpha}{\tau_\alpha s + 1}, \tag{4}$$

where $\bar{\alpha}(s)$ is the actuator command and k_α and τ_α are, respectively, the actuator gain and time constant. The latter two parameters can be obtained in bench tests. Section 4 shows the quadrotor dynamic response for two values of τ_α, simulating different tilting mechanism.

2.2 Gyroscopic Torque

The gyroscopic torque is created by the combination between the MAV attitude motion and the rotation of its propellers. It can be modeled in the $\mathcal{S}_\text{G}$ axes by Hughes (1986)

$$\mathbf{T}^g = I\sum_{i=1}^{4}(-1)^{i+1}\omega_i\mathbf{\Omega}\times\left(\mathbf{D}^\text{T}\begin{bmatrix}\sin\alpha\\ 0\\ \cos\alpha\end{bmatrix}\right), \tag{5}$$

where I is the moment of inertia of each propeller w.r.t. its rotation axis and $\mathbf{\Omega}$ is the angular velocity of $\mathcal{S}_\text{B}$ w.r.t. $\mathcal{S}_\text{G}$ represented in the $\mathcal{S}_\text{B}$ axes and $\mathbf{D}$ is the attitude matrix of $\mathcal{S}_\text{B}$ w.r.t. $\mathcal{S}_\text{G}$.

2.3 Attitude Motion

Attitude kinematics is modeled by Markley and Crassidis (2014)

$$\dot{\mathbf{D}} = -\mathbf{\Omega}\times\mathbf{D}, \tag{6}$$

Now assume that the vehicle has a rigid structure and $\mathcal{S}_\text{G}$ is an inertial frame. Moreover, consider the control torque $\mathbf{T}^c$, the gyroscopic torque in (11), and an arbitrary disturbance torque $\mathbf{T}^d$. Therefore, using the Newton-Euler formulation, the attitude dynamics of the MAV can be obtained in the $\mathcal{S}_\text{B}$ axes as

$$\dot{\mathbf{\Omega}} = \mathbf{J}^{-1}(\mathbf{J}\mathbf{\Omega})\times\mathbf{\Omega} + \mathbf{J}^{-1}\mathbf{T}^g + \mathbf{J}^{-1}\mathbf{T}^c + \mathbf{J}^{-1}\mathbf{T}^d, \tag{7}$$

where $\mathbf{J}$ is the body inertia matrix and the control torque $\mathbf{T}^c$ can be expressed in the $\mathcal{S}_\text{B}$ axes in terms of the individual thrust forces by

$$\mathbf{T}^c = \begin{bmatrix} -l\cos\alpha+\kappa\sin\alpha & -l\cos\alpha-\kappa\sin\alpha & l\cos\alpha+\kappa\sin\alpha & l\cos\alpha-\kappa\sin\alpha\\ -l\cos\alpha & l\cos\alpha & l\cos\alpha & -l\cos\alpha\\ \kappa\cos\alpha & -\kappa\cos\alpha & \kappa\cos\alpha & -\kappa\cos\alpha \end{bmatrix}\mathbf{f}, \tag{8}$$

where $\mathbf{f} \triangleq \begin{bmatrix} f_1 & f_2 & f_3 & f_4 \end{bmatrix}^\text{T}$, l is the arm length, $\kappa \triangleq k_\tau/k_f$, and α is the tilting angle.

Due to the maximum thrust force each rotor can support, there must be a saturation function to limit the torque. The vector with the maximum torque components that can be applied to this MAV with tilted rotors is

$$\mathbf{T}_{\max} = \begin{bmatrix} 2l\cos\alpha \\ 2l\cos\alpha \\ 2\kappa\cos\alpha \end{bmatrix}^T (\zeta_{\max} - \zeta_{\min}), \tag{9}$$

where

$$(\zeta_{\min}, \zeta_{\max}) = \begin{cases} \left(\bar{f}_{\min}, \frac{\bar{F}}{2} - \bar{f}_{\min}\right), & \text{if } \frac{\bar{F}}{2} - \bar{f}_{\min} < \bar{f}_{\max} \\ \left(\frac{\bar{F}}{2} - \bar{f}_{\max}, \bar{f}_{\max}\right), & \text{if } \frac{\bar{F}}{2} - \bar{f}_{\min} \geq \bar{f}_{\max} \end{cases} \tag{10}$$

$\bar{f}_{min}$ and $\bar{f}_{max}$ are respectively the minimum and maximum forces of each rotor and $\bar{F}_m$ is the thrust force necessary to support the hovercraft weight. Naturally the minimum torque components are given by $\mathbf{T}_{\min} = -\mathbf{T}_{\max}$.

2.4 Translational Motion

The vehicle's translational kinematics and dynamics are described in the $\mathcal{S}_{\mathrm{G}}$ axes by

$$\dot{\mathbf{r}} = \mathbf{v}, \tag{11}$$

$$\dot{\mathbf{v}} = \mathbf{g}_{\mathrm{G}} + \frac{1}{m}\mathbf{D}^{\mathrm{T}}\left(\mathbf{F}^c + \mathbf{F}^d\right) \tag{12}$$

where m is the vehicle's mass, $\mathbf{g}_{\mathrm{G}} \triangleq \begin{bmatrix} 0 & 0 & -g \end{bmatrix}^T$ is the gravitational acceleration vector and $\mathbf{F}^c$ are respectively arbitrary disturbance force and resulting control force in $\mathcal{S}_{\mathrm{B}}$ axes, which can be expressed in the in terms of the individual thrust forces by

$$\mathbf{F}^c = \begin{bmatrix} \sin\alpha \\ 0 \\ \cos\alpha \end{bmatrix} \sum_{i=1}^{4} f_i. \tag{13}$$

3 FLIGHT CONTROL SYSTEM

Assuming a time-scale separation between a faster attitude dynamics and a slower position dynamics, the conventional architecture for the flight control of multirotor aerial vehicles is an hierarchical scheme as illustrated in Figure 2 Bertrand et al. (2011). In this architecture, the inner loop is responsible for the attitude control while the outer one realizes the position tracking. The position controller receives a position command $\bar{\mathbf{r}} \in \mathbb{R}^3$ and uses feedback of position $\mathbf{r}$ and velocity $\mathbf{v}$ to compute a force command $\bar{\mathbf{F}}^c \in \mathbb{R}^3$. The attitude controller receives a three-dimensional attitude command represented by the combination of a heading command $\bar{\psi} \in \mathbb{R}$, a zero pitch command $\bar{\theta} \equiv 0$, and a roll command $\bar{\phi} = \sin^{-1}\left(\mathbf{e}_2^{\mathrm{T}}\bar{\mathbf{F}}^c\right)$. Then it uses feedback from attitude $\mathbf{D}$ and angular velocity $\boldsymbol{\Omega}$ to generate a torque command $\bar{\mathbf{T}}^c \in \mathbb{R}^3$. Both effort commands $\bar{\mathbf{F}}^c$ and $\bar{\mathbf{T}}^c$ are considered in the control allocation block to compute the effector commands, which are the inclination command $\bar{\alpha}$ and the four rotor commands $\bar{f}_i, i = 1, ..., 4$.

The time-scale separation assumption allows to separately design the attitude and the position controllers, as carried out in the sequel.

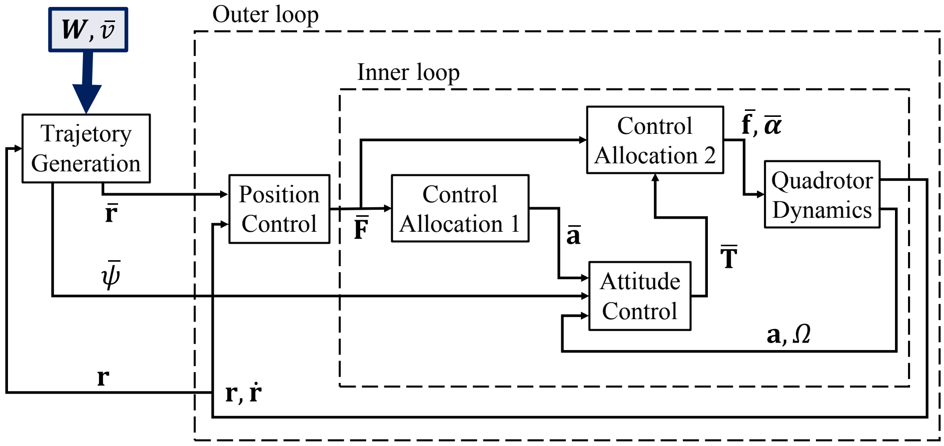

Figure 2: Structure of the MAV control system.

3.1 Attitude Control Law

For the purpose of designing the attitude control law, let us consider the parameterization of $\mathbf{D}$ by the Euler angles in the 3-2-1 sequence, which we denote by $\mathbf{a} \triangleq [\phi \;\; \theta \;\; \psi]^{\mathrm{T}}$. Assuming that $\mathbf{J}_{\mathrm{B}}$ is given by

$$\mathbf{J}_{\mathrm{B}} = \begin{bmatrix} J & 0 & 0 \\ 0 & J & 0 \\ 0 & 0 & J_z \end{bmatrix}, \tag{14}$$

the pitch θ and roll ϕ angles are close to zero, the Z_{B} angular velocity component $\mathbf{e}_3^{\mathrm{T}}\boldsymbol{\Omega}$ is zero whenever its other two components are different form zero and vice versa, and neglecting the disturbance torques, the following design model can be obtained

$$\dot{\mathbf{x}}_1^a = \mathbf{x}_2^a, \tag{15}$$

$$\dot{\mathbf{x}}_2^a = \mathbf{u}^a, \tag{16}$$

where $\mathbf{x}_1^a \triangleq \mathbf{a}$, $\mathbf{x}_2^a \triangleq \boldsymbol{\Omega}^{\mathrm{T}}$ and $\mathbf{u}^a \triangleq \mathbf{J}_{\mathrm{B}}^{-1}\bar{\mathbf{T}}^c \in \mathbb{R}^3$.

To complete the above design model, one must account for the saturation that need to be imposed to the torque command $\bar{\mathbf{T}}^c$. The particular torque bounds appropriate for the MAV under consideration are presented by equations (9) and (10), therefore $\mathbf{u}^a$ is bounded in a parallelepipedal set with extreme corners denoted by $\mathbf{u}^a_{\min} \in \mathbb{R}^3$ and $\mathbf{u}^a_{\max} \in \mathbb{R}^3$.

Now, on the basis of the above model, we propose the following attitude control law:

$$\mathbf{u}^a = \sigma_{[\mathbf{u}^a_{\min}, \mathbf{u}^a_{\max}]}\left(\mathbf{K}^a_p \boldsymbol{\varepsilon}^a - \mathbf{K}^a_d \boldsymbol{\Omega}\right), \tag{17}$$

where $\mathbf{K}^a_p \in \mathbb{R}^{3\times3}$ is a proportional gain, $\mathbf{K}^a_d \in \mathbb{R}^{3\times3}$ is a derivative gain, $\boldsymbol{\varepsilon}^a \in \mathbb{R}^3$ are the Euler angles corresponding to attitude control error $\tilde{\mathbf{D}} \triangleq \bar{\mathbf{D}}\mathbf{D}^{\mathrm{T}}$, and $\sigma_{[\mathbf{u}^a_{\min}, \mathbf{u}^a_{\max}]} : \mathbb{R}^3 \to \mathbb{R}^3$ whose ith component is given by

$$\sigma_{[u^a_{\min,i}, u^a_{\max,i}]}(\gamma) \triangleq \begin{cases} u^a_{\max,i} & , \quad \gamma > u^a_{\max,i} \\ \gamma & , \quad \gamma \in [u^a_{\min,i}, u^a_{\max,i}] \\ u^a_{\min,i} & , \quad \gamma < u^a_{\min,i} \end{cases}. \tag{18}$$

The closed loop system (15)-(17) is a double integrator controlled by a linear saturated control law. Tyan and Bernstein (1999) studied the stability of such a system, showing that under conventional detectability and observability conditions, it is globally asymptotically stable. Moreover, one can see that in saturation-free conditions, (15)-(17) is a standard second order linear time-invariant system, whose dynamics can be exactly designed to cope with specified time response and overshoot.

From the definition of $\mathbf{u}^a$ (after equation (16)), one can immediately obtain the torque command $\bar{\mathbf{T}}^c = \mathbf{J}_{\mathrm{B}}\mathbf{u}^a$.

3.2 Position Control Law

Now consider the true model (11)-(12) of the translational motion. By neglecting the disturbance force $\mathbf{F}^d$ and assuming that the attitude command $\bar{\mathbf{D}}$ is equal to the actual attitude $\mathbf{D}$ (time-scale separation assumption), the design model for the position controller is also obtained as a double integrator:

$$\dot{\mathbf{x}}^p_1 = \mathbf{x}^p_2, \tag{19}$$

$$\dot{\mathbf{x}}^p_2 = \mathbf{u}^p, \tag{20}$$

where $\mathbf{x}^p_1 \triangleq \mathbf{r}$, $\mathbf{x}^p_2 \triangleq \mathbf{v}$, $\mathbf{u}^p \triangleq \mathbf{g}_{\mathrm{G}} + \frac{1}{m}\bar{\mathbf{F}}^c$.

The force command $\bar{\mathbf{F}}^c$ is assumed to be bounded inside a parallelepipedal set $\mathbf{F}_{\min} \leq \bar{\mathbf{F}}^c \leq \mathbf{F}_{\max}$. Therefore, from the above definition of the virtual control input $\mathbf{u}^p$, one can find its admissible set to be $\mathbf{u}^p_{\min} \leq \mathbf{u}^p \leq \mathbf{u}^p_{\max}$, where

$$\mathbf{u}^p_{\min} \triangleq \mathbf{g}_{\mathrm{G}} + \frac{1}{m}\mathbf{F}_{\min} \quad \text{and} \quad \mathbf{u}^p_{\max} \triangleq \mathbf{g}_{\mathrm{G}} + \frac{1}{m}\mathbf{F}_{\max}. \tag{21}$$

The above design model is of the same type as the one adopted in subsection 3.1 to design the attitude control law. Therefore, we similarly propose a linear saturated controller for the position control loop, i.e.,

$$\mathbf{u}^p = \sigma_{[\mathbf{u}^p_{\min},\mathbf{u}^p_{\max}]}\left(\mathbf{K}^p_p\boldsymbol{\varepsilon}^p - \mathbf{K}^p_d\mathbf{v}\right), \tag{22}$$

where $\mathbf{K}^p_p \in \mathbb{R}^{3\times3}$ is a proportional gain, $\mathbf{K}^p_d \in \mathbb{R}^{3\times3}$ is a derivative gain, $\boldsymbol{\varepsilon}^p \triangleq \bar{\mathbf{r}} - \mathbf{r}$ is the position control error.

From the definition of $\mathbf{u}^p$ (after equation (20)), one can immediately obtain the force command $\bar{\mathbf{F}}^c = m(\mathbf{u}^p - \mathbf{g}_\mathrm{G})$.

3.3 Control Allocation

From the effort commands $\bar{\mathbf{T}}^c$ and $\bar{\mathbf{F}}^c$ computed by the above attitude and position controllers, one must provide the effective commands of the flight control system depicted in Figure 2. Namely, those are the attitude command and the motor commands.

Attitude Commands (Control Allocation 1)

In the proposed system, the vehicle's attitude is primarily intended to be controlled to follow an external heading command $\bar{\psi} \in \mathbb{R}$ and to regulate the pitch angle to zero. In order to attend the resultant thrust command $\bar{\mathbf{F}}^c$ in $\mathrm{Y_B}$ direction a roll angle command $\bar{\phi} \in \mathbb{R}$ must be applied to the inner (attitude control) loop. From the geometry of the thrust force in $\mathrm{Y_B} - \mathrm{Z_B}$ plane the roll angle command is given by,

$$\bar{\phi} = \cos^{-1}\frac{\bar{F}_z}{\sqrt{\bar{F}_y^2 + \bar{F}_z^2}} \tag{23}$$

where $\bar{F}_x \triangleq \mathbf{e}_1^\mathrm{T}\bar{\mathbf{F}}^c$, $\bar{F}_y \triangleq \mathbf{e}_2^\mathrm{T}\bar{\mathbf{F}}^c$, $\bar{F}_z \triangleq \mathbf{e}_3^\mathrm{T}\bar{\mathbf{F}}^c$. Therefore, the three-dimensional attitude command can by computed by $\bar{\mathbf{D}}^{\mathrm{B/G}} = \mathbf{D}_3(\bar{\psi})\mathbf{D}_1(\bar{\phi})$, with

$$\mathbf{D}_1(\bar{\phi}) = \begin{bmatrix} 1 & 0 & 0 \\ 0 & \mathrm{c}\bar{\phi} & \mathrm{s}\bar{\phi} \\ 0 & -\mathrm{s}\bar{\phi} & \mathrm{c}\bar{\phi} \end{bmatrix} \quad \text{and} \quad \mathbf{D}_3(\bar{\psi}) = \begin{bmatrix} \mathrm{c}\bar{\psi} & \mathrm{s}\bar{\psi} & 0 \\ -\mathrm{s}\bar{\psi} & \mathrm{c}\bar{\psi} & 0 \\ 0 & 0 & 1 \end{bmatrix}. \tag{24}$$

Rotors and Tilting Angle Commands (Control Allocation 2)

Since the pitch command is regulated to zero, in order to attend the resultant thrust command $\bar{\mathbf{F}}^c$ in $\mathrm{X_B}$ direction, an inclination angle command $\bar{\alpha} \in \mathbb{R}$ must be sent to the servomotor. Analogously to the roll command angle, from the geometry of the thust force in $\mathrm{X_B} - \mathrm{Z_B}$ plane, the tilting angle command is given by,

$$\bar{\alpha} = \cos^{-1}\frac{\bar{F}_z}{\sqrt{\bar{F}_x^2 + \bar{F}_z^2}} \tag{25}$$

From $\bar{\mathbf{F}}^c$, one can immediately obtain the thrust magnitude command to be $\bar{F} = \|\bar{\mathbf{F}}^c\|$. By replacing the effective efforts in equation (8) by the respective commands and noting that $\bar{F} = \sum_{i=1}^{4} \bar{f}_i$, one can write

$$\begin{bmatrix} \bar{F} \\ \bar{\mathbf{T}}^c \end{bmatrix} = \begin{bmatrix} 1 & 1 & 1 & 1 \\ -l\cos\bar{\alpha} + \kappa\sin\bar{\alpha} & -l\cos\bar{\alpha} - \kappa\sin\bar{\alpha} & l\cos\bar{\alpha} + \kappa\sin\bar{\alpha} & l\cos\bar{\alpha} - \kappa\sin\bar{\alpha} \\ -l\cos\bar{\alpha} & l\cos\bar{\alpha} & l\cos\bar{\alpha} & -l\cos\bar{\alpha} \\ \kappa\cos\bar{\alpha} & -\kappa\cos\bar{\alpha} & \kappa\cos\bar{\alpha} & -\kappa\cos\bar{\alpha} \end{bmatrix} \bar{\mathbf{f}}, \tag{26}$$

where $\bar{\mathbf{f}} \triangleq [\bar{f}_1\ \bar{f}_2\ \bar{f}_3\ \bar{f}_4]^{\mathrm{T}}$, Given the tilting angle command $\bar{\alpha}$, equation (26) is a well-posed linear system of equations. Therefore, the rotor commands $\bar{\mathbf{f}}$ can be uniquely allocated by inverting this equation.

3.4 Trajectory Generation

In order to make the vehicle follow a waypoint-based path with a desired speed and with its longitudinal axis pointing toward the next waypoint of the sequence, a heading command and a position command need to be generated accordingly.

For a desired speed $\bar{v}$ and a given waypoint sequence $W \triangleq \{\mathbf{w}^1, \mathbf{w}^2, ..., \mathbf{w}^k\}$, where $\mathbf{w}^j \in \mathbb{R}^3$, for $j = 1, 2, ..., k$, the position command between a waypoint j and the following $j+1$ is here defined as

$$\bar{\mathbf{r}} \triangleq \mathbf{w}^j + \frac{\mathbf{w}^{j+1} - \mathbf{w}^j}{||\mathbf{w}^{j+1} - \mathbf{w}^j||}\bar{v}\Delta t, \tag{27}$$

where Δt stands for the time difference from the instant where $\bar{\mathbf{r}} = \mathbf{w}^j$. In words, it means that the MAV is commanded to move in a straight line with a desired speed $\bar{v}$ from one point $\mathbf{w}^j$ to the next one $\mathbf{w}^{j+1}$.

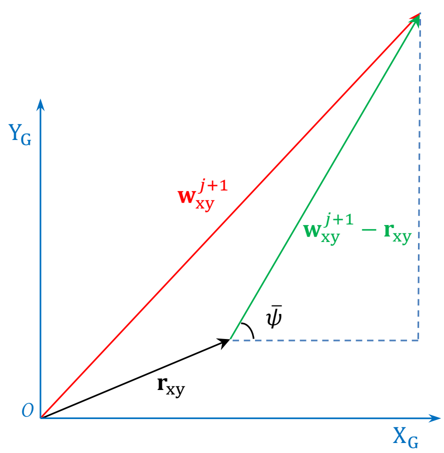

Figure 3: Heading command definition.

Denote the $\mathrm{X_G} - \mathrm{Y_G}$ projection of the position $\mathbf{r}$ and a given waypoint $\mathbf{w}^j$ by $\mathbf{r}_{xy}$ and

$\mathbf{w}_{\text{xy}}^{j}$, respectively. The heading command is generated by

$$\bar{\psi} \triangleq \begin{cases} \cos^{-1}\left(\mathbf{e}_1^{\mathrm{T}} \frac{\mathbf{w}_{\text{xy}}^{j+1} - \mathbf{r}_{\text{xy}}}{||\mathbf{w}_{\text{xy}}^{j+1} - \mathbf{r}_{\text{xy}}||}\right) & , \ ||\mathbf{w}_{\text{xy}}^{j+1} - \mathbf{r}_{\text{xy}}|| > d_{\min} \\ \cos^{-1}\left(\mathbf{e}_1^{\mathrm{T}} \frac{\mathbf{w}_{\text{xy}}^{j+2} - \mathbf{r}_{\text{xy}}}{||\mathbf{w}_{\text{xy}}^{j+2} - \mathbf{r}_{\text{xy}}||}\right) & , \ ||\mathbf{w}_{\text{xy}}^{j+1} - \mathbf{r}_{\text{xy}}|| \leq d_{\min} \end{cases}, \tag{28}$$

where $d_{\min}$ is a trajectory design parameter. Figure 3 illustrates how $\bar{\psi}$ is defined.

4 SIMULATION-BASED EVALUATION

This section presents a computational simulation of the proposed flight control system using MATLAB/Simulink. The simulation environment is described in Subsection 4.1 and the results are presented in Subsection 4.2 along with comments.

4.1 Simulation Description

The MAV here considered has a mass $m = 1$ kg, arm length of $l = 0.183$ m, inertia matrix $\mathbf{J}_{\text{B}} = \text{diag}\{0.02, 0.02, 0.03\}$ kgm^2. The motor drive has a time constant of $\tau_m = 0.01$ s and a unitary gain $k_m = 1$, the propellers force and torque constants are, respectively, $k_f = 3.13 \times 10^{-5}$ N/(rad/s)^2 and $k_\tau = 7.5 \times 10^{7}$ Nm/(rad/s)^2 and its moment of inertia $I = 10^{-4}$kgm^2. Two tilting actuator are analyzed, both with unitary gains $k_\alpha = 1$, but different time constants, one with $\tau_\alpha = 1$ s and the other with $\tau_\alpha = 0.01$ s. The minimum and maximum values for the individual thrust forces considered are $f_{\min} = 2$ N and $f_{\max} = 20$ N.

The attitude control gains ($\mathbf{K}_p^a = \text{diag}\{20\ 20\ 20\}$ and $\mathbf{K}_d^a = \text{diag}\{8\ 8\ 8\}$) and the position control gains ($\mathbf{K}_p^p = \text{diag}\{20\ 20\ 20\}$ and $\mathbf{K}_d^p = \text{diag}\{10\ 10\ 10\}$) are chosen using pole placement.

The adopted waypoint sequence is $W = \left\{[0\ 0\ 0]^{\mathrm{T}}, [0\ 0\ 20]^{\mathrm{T}}, [0\ 20\ 20]^{\mathrm{T}}, [20\ 20\ 20]^{\mathrm{T}}\right\}$. Two commanded velocities are studied, $\bar{v} = 1$ m/s and $\bar{v} = 5$ m/s. The trajectory design parameter is set to $d_{\min} = 2$ m.

4.2 Simulation Results and Comments

First let us present the results when the commanded velocity is $\bar{v} = 1$ m/s.

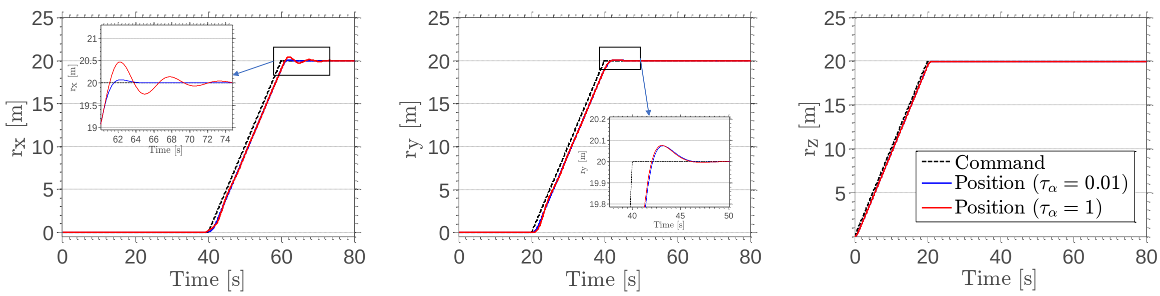

Figure 4: Position of the quadrotor when traveling at commanded velocity $\bar{v} = 1$ m/s.

Figure 4 presents the position graphics. In the Z_G axis there are no overshoot, and the accommodation time is around 1.4 s; in the Y_G the difference when using a fast or a slow tilting mechanism is imperceptible. The overshoot is of 0.08 m and the accommodation time of 4.8 s; in the X_G axis, the difference between the two tilting dynamic response is noticeable. The blue curve has an overshoot of 0.07 m and a accommodation time of around 3.6 s. For the slow tilting mechanism, these values are 0.47 m and 14.2 s. Figure 5 shows that, for this commanded speed, the MAV is able to move almost horizontally, with $|\phi| < 4$ deg and $|\theta| < 1.1$ deg. ψ goes from zero to 90 deg and then goes back to zero, allowing the MAV to move most of the time along the X_B axis.

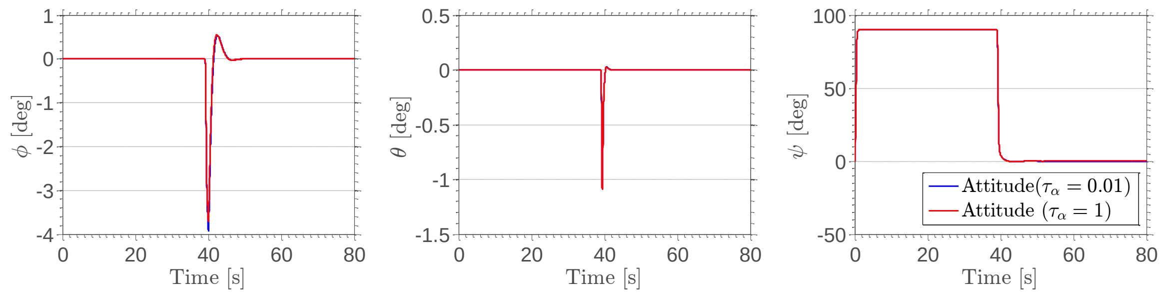

Figure 5: Attitude of the quadrotor when traveling at commanded velocity $\bar{v} = 1$ m/s.

Figures 6 and 7 show the torque components and the thrust force applied by the propellers on the MAV. Figure 8 presents α, showing that the overshoot and the accommodation time are higher for the vehicle with the slower tilting dynamics. Figure 9 shows that, with both values of τ_α, the horizontal trajectory of the MAV is very close to the desired path.

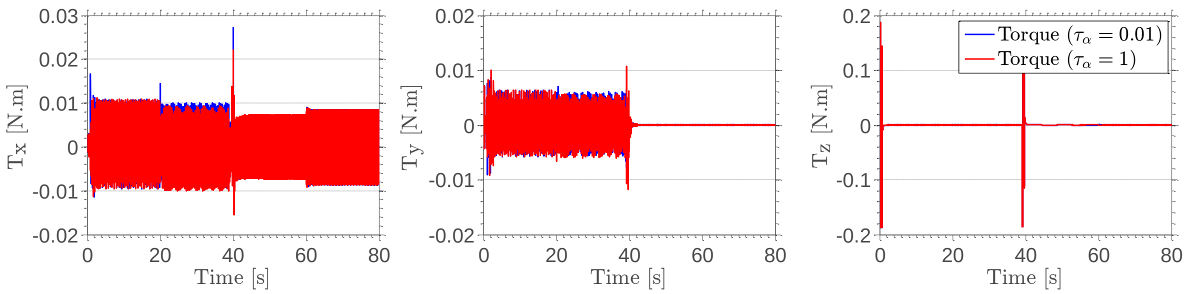

Figure 6: Torque applied by the propellers when traveling at commanded velocity $\bar{v} = 1$ m/s.

The following figures present the results for the task with the desired speed $\bar{v} = 5$ m/s. Figure 10 shows the position graphics. In X_G the position overshoot and accommodation time go from 0.35 m and 4.2 s when $\tau_\alpha = 0.01$ s, to 2.6m and 17.4 s when $\tau_\alpha = 1$ s, respectively. In Y_G, when $\tau_\alpha = 0.01$ s, the overshoot is 0.7 m and the accommodation time is 7.5 s, on the other hand, when $\tau_\alpha = 1$ s, the overshoot in Y_G axis is increased to 1.4 m and the accommodation time to 9.2 s. In Z_G there is no difference, both present no overshoot and an accommodation time of 2.5s.

Figure 11 shows that, even with commanded velocity of $\bar{v} = 5$ m/s, the MAV is able to fly almost aligned to the horizontal. For the faster tilting dynamic, ϕ is always less

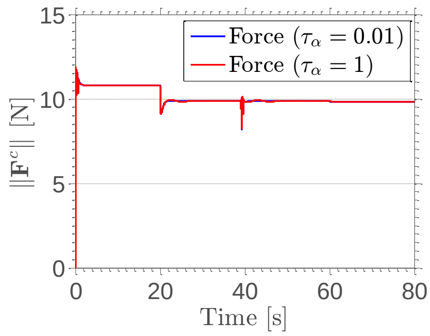

Figure 7: Thrust force applied by the propellers when traveling at commanded velocity $\bar{v} = 1$ m/s.

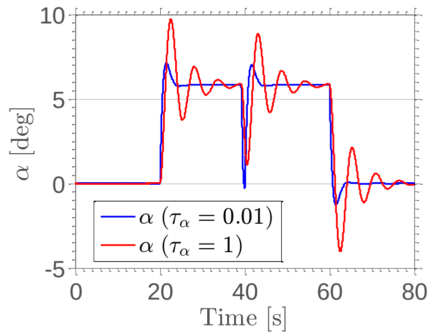

Figure 8: Tilt angle α of the rotors for commanded velocity $\bar{v} = 1$ m/s.

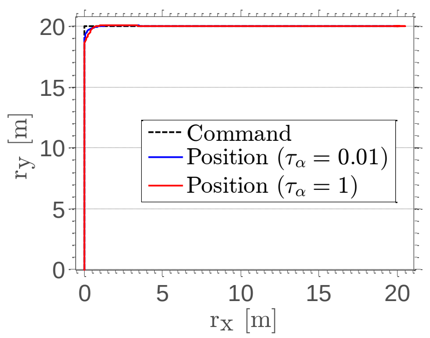

Figure 9: Horizontal path of the MAV for commanded velocity $\bar{v} = 1$ m/s.

than 5 deg and θ less than 3.5 deg, for $\tau_\alpha = 1$ s the maximum value of ϕ is around 11 deg and $\theta < 5.5$ deg. As well as on the first task, ψ changes in order to head the MAV to the desired position, making it move mainly along the X_B axis.

Figure 12 and 13 show the torque and the thrust force applied by the propellers on the MAV. There is torque saturation in Z_B. The tilt angle α is presented in Figure 14 for the two tilting dynamics. Figure 15 shows that, when flying at the velocity of 5 m/s, there is a higher deviation from the desired path on $X_B - Y_B$ plane, but the quadrotor still reaches the waypoints successfully.

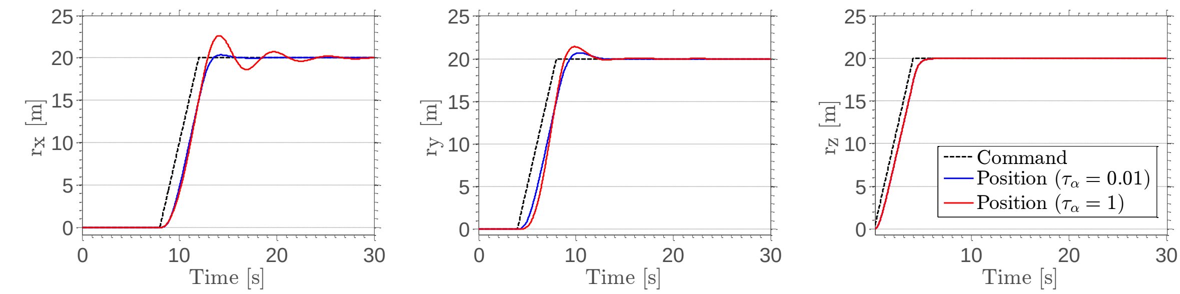

Figure 10: Position of the quadrotor when traveling at commanded velocity $\bar{v} = 5$ m/s.

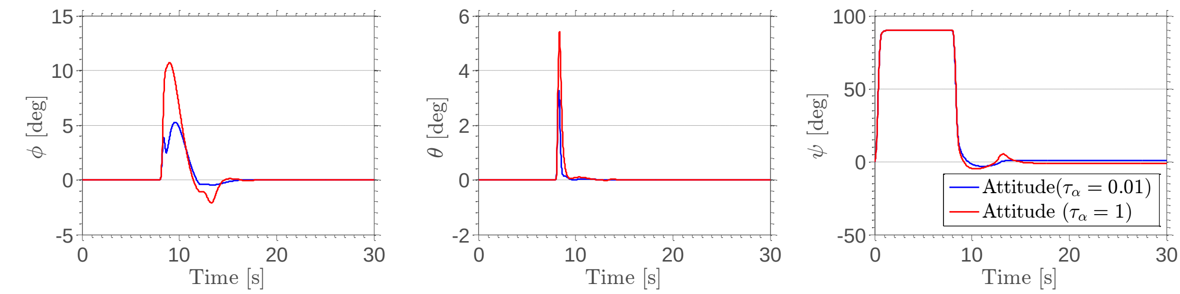

Figure 11: Attitude of the quadrotor when traveling at commanded velocity $\bar{v} = 5$ m/s.

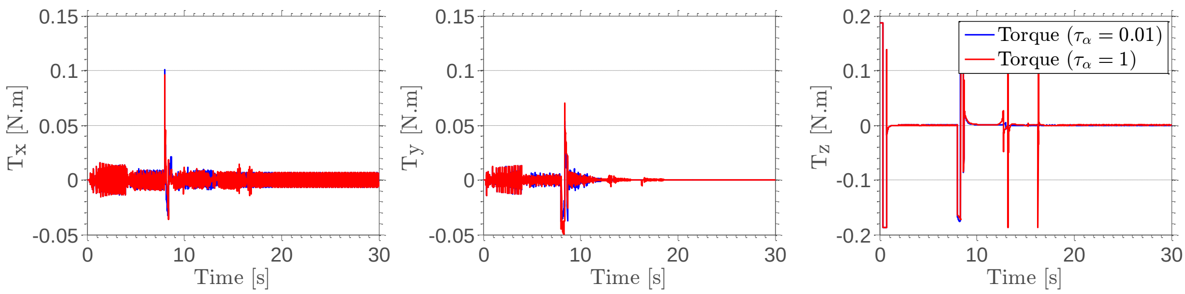

Figure 12: Torque applied by the propellers when traveling at commanded velocity $\bar{v} = 5$ m/s.

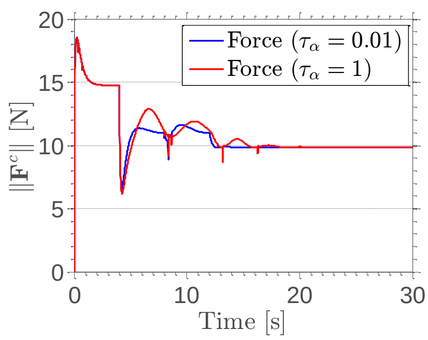

Figure 13: Thrust force applied by the propellers when traveling at commanded velocity $\bar{v} = 5$ m/s.

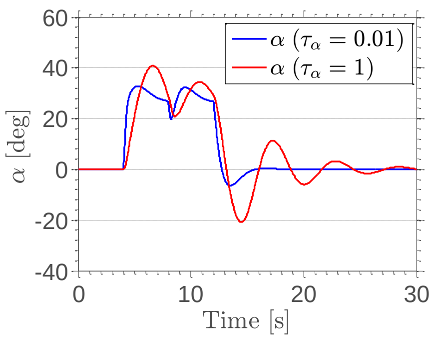

Figure 14: Tilt angle α of the rotors for commanded velocity $\bar{v} = 5$ m/s.

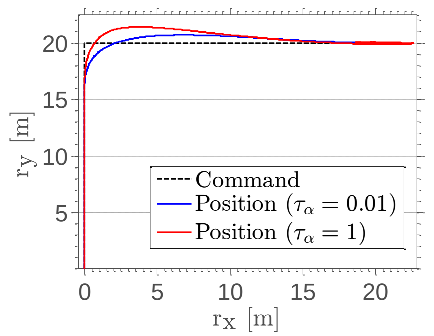

Figure 15: Horizontal path of the MAV for commanded velocity $\bar{v} = 5$ m/s.

5 CONCLUSIONS

The paper presented the dynamic modeling and flight control design of an MAV with rotors that can be commanded to tilt frontward and backward continuously. This vehicle is designed in such a way that the pitch angle is regulated to zero, while the rotors are tilted to control the longitudinal translation. The lateral translation is controlled just as the conventional multirotor vehicles, using differential thrust commands. A trajectory generation strategy appropriate for the new vehicle is also presented. It provides a waypoint-based trajectory with the heading command defined in such a way that the front side of the MAV points at the flight direction.

The proposed system was evaluated on the basis of deterministic simulations, under different speed commands and tilting-mechanism time responses. The results showed that the quadcopter with longitudinal tilting rotors is able to track a waypoint-based trajectory with good accuracy, keeping the roll and pitch angles close to zero.

ACKNOWLEDGEMENTS

The first author would like to thank CAPES for the master scholarship to support this investigation. The second author are also greatful to FAPESP (grant 2015/04393-2) and CNPq (grant 475251/2013-0) for supporting the Laboratório de Robótica Aérea of the Aeronautics Institute of Technology.

REFERENCES

Sylvain Bertrand, Nicolas Guénard, Tarek Hamel, Hélène Piet-Lahanier, and Laurent Eck. A hierarchical controller for miniature VTOL UAVs: Design and stability analysis using singular perturbation theory. *Control Engineering Practice*, 19(10):1099–1108, 2011. ISSN 09670661. doi: 10.1016/j.conengprac.2011.05.008.

S. Bouabdallah and R. Siegwart. Backstepping and sliding-mode techniques applied to an indoor micro quadrotor. In *IEEE International Conference on Robotics and Automation*, 2005.

Hanoch Efraim, Amir Shapiro, and Gera Weiss. Quadrotor with a dihedral angle: on the effects of tilting the rotors inwards. *Journal of Intelligent & Robotic Systems*, 80(2):313–324, 2015. ISSN 1573-0409. doi: 10.1007/s10846-015-0176-4. URL `http://dx.doi.org/10.1007/s10846-015-0176-4`.

J. Escareno, A. Sanchez, O. Garcia, and R. Lozano. Triple tilting rotor mini-uav: Modeling and embedded control of the attitude. In *American Control Conference*, pages 3476–3481, Seattle, USA, June 2008.

H.Bouadi, M.Bouchoucha, and M.Tadjine. Modelling and stabilizing control laws design based on sliding mode for an uav type-quadrotor. *Engineering Letters*, 2007.

Peter C. Hughes. *Spacecraft Attitude Dynamics*. Dover Publications, 1986.

Robert Mahony, Vijay Kumar, and Peter Corke. Multirotor aerial vehicles: Modeling, estimation, and control of quadrotor. *IEEE Robotics & Automation Magazine*, 19(3):20–32, 2012.

F. L. Markley and J. L. Crassidis. *Fundamentals of Spacecraft Attitude Determination and Control*. Space Technology Library, 2014.

Mohamed Kara Mohamed and Alexander Lanzon. Design and control of novel tri-rotor uav. In *UKACC International Conference on Control*, pages 304–309, Cardiff, UK, September 2012.

Kaan T. Oner, Ertugrul Cetinsoy, Mustafa Unel, Mahmut F. Aksit, Ilyas Kandemir, and Kayhan Gulez. Dynamic model and control of a new quadrotor unmanned aerial vehicle with tilt-wing mechanism. *International Journal of Mechanical, Aerospace, Industrial, Mechatronic and Manufacturing Engineering*, 2008.

Paul Edward Ian Pounds. *Design, Construction and Control of a Large Quadrotor Micro Air Vehicle*. PhD thesis, Australian National University, 2007.

Davi A. Santos, O. Saotome, and A. Cela. Trajectory control of multirotor helicopters with thrust vector constraints. In *21st Mediterranean Conference on Control and Automation (MED)*, pages 375–379, Chania, Greece, June 2013.

Pau Segui-Gasco, Yazan Al-Rihani, Hyo-Sang Shin, and Al Savvaris. A novel actuation concept for a multi rotor uav. *J Intell Robot Syst*, 2014.

F. Tyan and D. S. Bernstein. Global stabilization of systems containing a double integrator using saturated linear controller. *International Journal of Robust and Nonlinear Control*, 9(1999):1143–1156, 1999.